Molecular BioSystems

www.molecularbiosystems.org

Volume 7 | Number 7 | 1 July 2011 | Pages 2089–2332

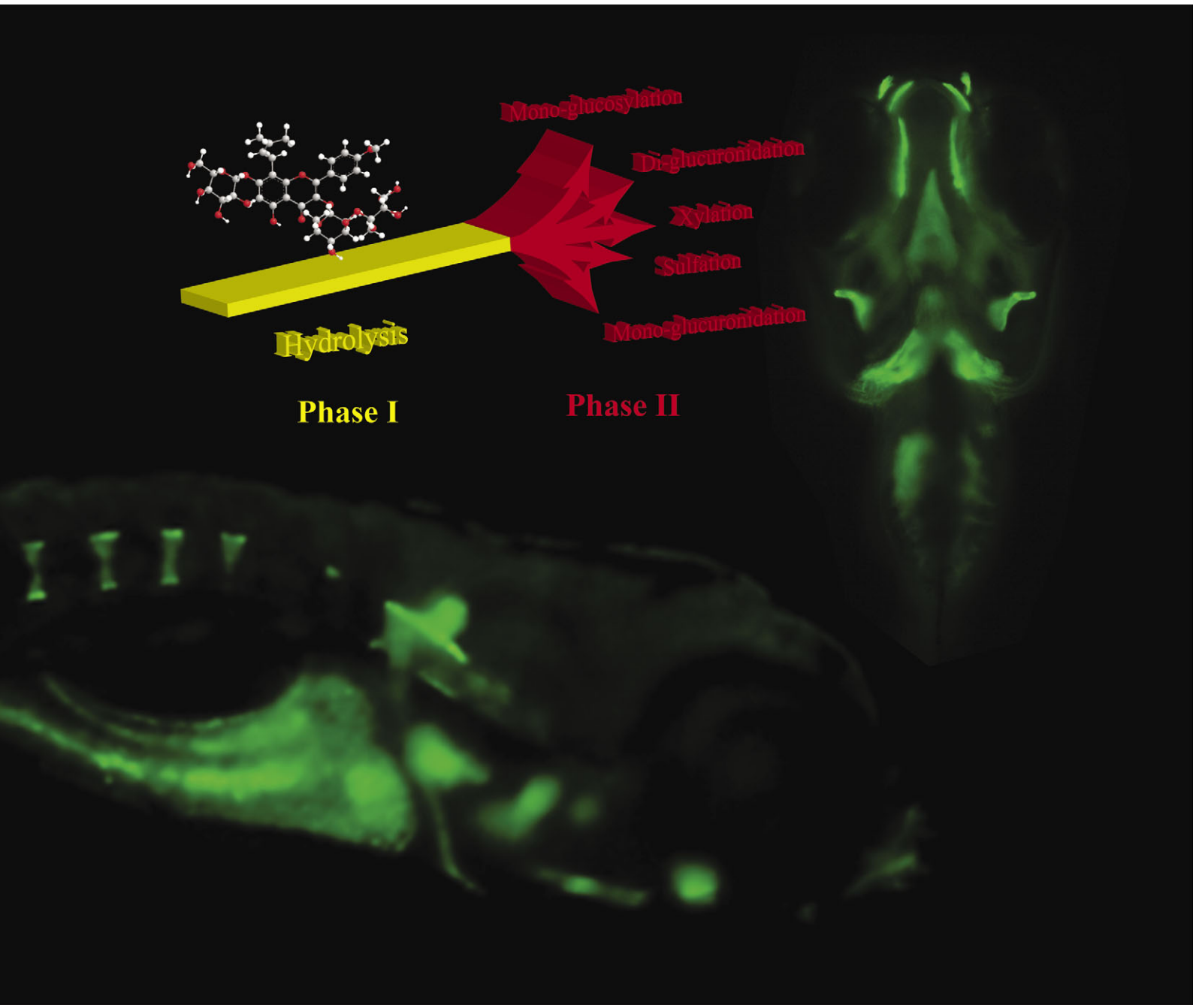

ISSN 1742-206X

RSC Publishing

PAPER

Simon Ming-Yuen Lee *et al.*

Combined *in vivo* imaging and omics approaches reveal metabolism of icaritin and its glycosides in zebrafish larvae

Molecular BioSystems

Dynamic Article Links

Cite this: *Mol. BioSyst.*, 2011, **7**, 2128–2138

www.rsc.org/molecularbiosystems

PAPER

Combined *in vivo* imaging and omics approaches reveal metabolism of icaritin and its glycosides in zebrafish larvae

Zhen Hua Li,†[a] Deepa Alex,†[a] Shiu On Siu,†[ab] Ivan Keung Chu,[b] Joerg Renn,[c] Christoph Winkler,[c] Shaoke Lou,[de] Stephen Kwok-Wing Tsui,[de] Hai Yu Zhao,[a] Wendy Ru Yan,[a] Gail B. Mahady,[f] Guo Hui Li,[b] Yiu Wa Kwan,[d] Yi Tao Wang[a] and Simon Ming-Yuen Lee*[a]

Received 3rd January 2011, Accepted 8th March 2011
DOI: 10.1039/c1mb00001b

Flavonoids isolated from *Herba Epimedii* such as icaritin, icariin and epimedin C have been suggested as potential bone anabolic compounds. However, the "specific localized effects" of these flavonoids in bone, *in vivo*, and the metabolism of these flavonoids in zebrafish larvae have never been demonstrated. In this study, we used multiple methods including *in vivo* imaging, drug metabolites profiling, transcriptomic and proteomic approaches to determine the mechanisms involved in the distribution and metabolism of the flavonoids in zebrafish larvae by measuring the fluorescence emission, *in vivo*, of icaritin and its glycoside derivatives. The fluorescence emission mechanism of icaritin *in vitro* was identified by spectrophotometric analysis, and the fluorescent property of icaritin was used as a probe to visualize the metabolism and distribution of icaritin and its glycoside derivatives in zebrafish larvae. Phase I and phase II metabolism of icaritin and its derivatives were identified in zebrafish by mass spectrometry. The combined transcriptomics and proteomics demonstrate a high degree of conservation of phase I and phase II drug metabolic enzymes between zebrafish larvae and mammals. Icaritin and its glycoside derivatives were demonstrated using combined approaches of *in vivo* imaging, drug metabolites identification, and transcriptomic and proteomic profiling to illustrate phase I and phase II metabolism of the flavonoids and their distribution in bone of zebrafish larvae. This study provides a new methodological model for use of the zebrafish larvae to examine drug metabolism.

Introduction

Herba Epimedii is the dried aerial part of several *Epimedium* species,[1] which has been widely used in China as a medicinal herb for the treatment of infertility, impotence, osteoporosis and weakness of the limbs. Recent *in vitro* and *in vivo* studies have revealed that flavonoids isolated from *Epimedium* species have potential bone anabolic activities and inhibit osteoclastic bone resorption.[2] In a randomized, controlled clinical trial in postmenopausal women, *Herba Epimedii*-derived flavonoids consumption prevented bone loss.[3]

Herba Epimedii contains several flavonoid compounds, such as icaritin, icariin and epimedin C, with a common C-prenylated flavonol parent ring (Fig. 1A). Icariin, 3-[(6-deoxy-α-L-mannopyranosyl)oxy]-7-(β-D-glucopyranosyloxy)-5-hydroxy-2-(4-methoxyphenyl)-8-(3-methyl-2-buten-1-yl)-4*H*-1-benzopyran-4-one, is the major flavonoid constituent in the genus *Epimedium*. In mammalian models, *Herba Epimedii*-derived prenylated flavonoids with a monoglucosidic bond such as icariin are rapidly hydrolyzed during intestinal metabolism.[4–6]

Zebrafish have become one of the most popular animal models for drug screening because of the high degree of conservation of key signaling pathways and functional protein domains with human counterparts.[7–9] Since developmental and physiological processes are highly conserved between zebrafish and mammals, compounds designed to interact with numerous processes of interested in zebrafish usually elicit

[a] *State Key Laboratory of Quality Research of Chinese Medicine, Institute of Chinese Medical Sciences, University of Macau, Av. Padre Tomás Pereira S.J., Taipa, Macao, China. E-mail: SimonLee@umac.mo*
[b] *Department of Chemistry, The University of Hong Kong, 21 Sassoon Road, Pokfulam, Hong Kong, China*
[c] *Department of Biological Sciences, National University of Singapore, Singapore*
[d] *School of Biomedical Sciences, Faculty of Medicine, The Chinese University of Hong Kong, Hong Kong, China*
[e] *Hong Kong Bioinformatics Centre, The Chinese University of Hong Kong, Hong Kong, China*
[f] *Departments of Pharmacy Practice and Pan-American Health Organization/World Health Organization Collaborating Centre for Traditional Medicine, College of Pharmacy, University of Illinois at Chicago, Chicago, USA*
† Co-first authors contributed equally to the work.

comparable pharmacological effects in humans.[10–13] The use of zebrafish for drug screening as well as for various pharmacological studies has received increasing scientific interest in areas of drug absorption, metabolism, distribution and excretion.[14] However, there is a lack of detailed systematic studies investigating the fate of drugs after absorption as well as identification of the enzymes involved in drug metabolism in zebrafish larvae.

Thus, in the present study, we utilized techniques such as *in vivo* imaging, drug metabolite profiling, transcriptomic and proteomic approaches to investigate the mechanism(s) of distribution and metabolism of *Herba Epimedii*-derived flavonoids: icaritin, icariin and epimedin C, in zebrafish larvae. Given the fact that icaritin elicits a novel, bone-specific fluorescence in zebrafish, the real-time metabolism and distribution of icaritin and its glycoside derivatives could be evaluated by fluorescence microscopy in live, whole zebrafish larvae. In addition, metabolism of these compounds could be identified by liquid chromatography tandem mass spectrometry (LC-MS/MS) and drug-metabolizing enzymes expressed in zebrafish larvae were identified using transcriptomic and proteomic profiling by deep sequencing and reverse phase-reverse phase-two dimensional-liquid chromatography-tandem mass spectrometry (RP-RP-2D-LC-MS/MS), respectively. The combined omics approaches have been used to address metabolism of icaritin and its derivatives in zebrafish larvae.

Results

Icaritin elicits bone-specific fluorescence in zebrafish larvae

Prenylated flavonoids from *Herba Epimedii* have been reported possessing protective effects against bone loss in animal models and in human clinical trials. The deposition/accumulation of these flavonoids after consumption in bone, however, is unknown. In this study, we demonstrated that after treatment of zebrafish larvae with flavonoids of *Herba Epimedii*, fluorescence signals were detected in bone structures of the zebrafish larvae which are similar to that with locations of the bone-specific dye calcein (Fig. 1B). It has been reported that calcein stains mineralized bone specifically by binding with calcium to form a complex which emits green fluorescence upon excitation.[15] As shown in Fig. 2, icaritin-treated zebrafish larvae clearly demonstrated green fluorescence in the mineralized pharyngeal skull which is perfectly overlapping with the fluorescence of bone staining using calcein. The phenomenon of icaritin-induced bone-specific fluorescence suggested that icaritin and calcein might elicit fluorescence by similar mechanisms.

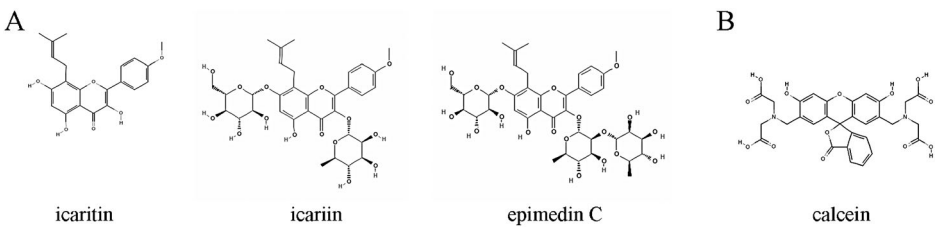

Fig. 1 (A) three major flavonoids (icaritin, icariin and epimedin C) identified in *Herba Epimedii* have the same parental 8-prenylkaempferol ring. (B) structure of bone-specific dye, calcein.

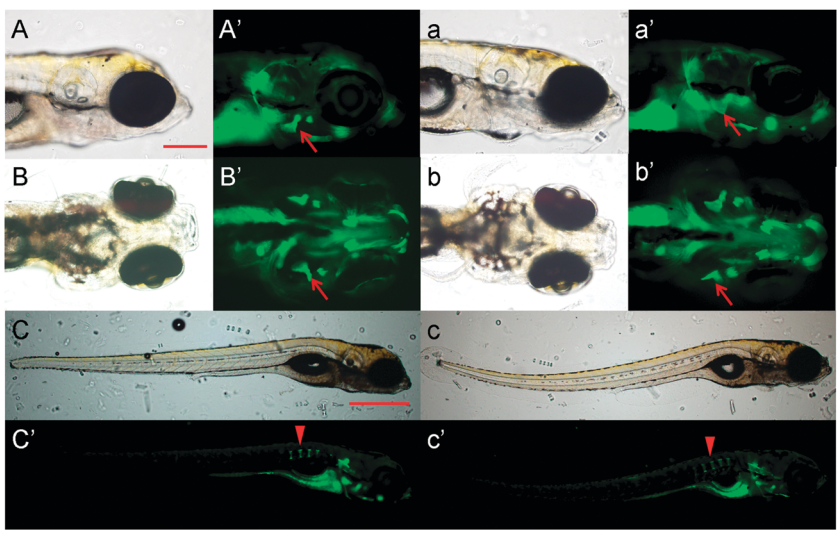

Fig. 2 Fluorescence in mineralized head bone of icaritin-treated 14 dpf zebrafish (A′–C′) similar to that observed with calcein staining (a′–c′). A and A′, lateral view of icaritin-treated 14 dpf zebrafish; a and a′, lateral view of 14 dpf zebrafish after staining with calcein; B and B′, ventral view of icaritin-treated 14 dpf zebrafish; b and b′, ventral view of 14 dpf zebrafish after calcein staining; C and C′, lateral view of the whole body of icaritin-treated 14 dpf zebrafish; c and c′, lateral view of the whole body of 14 dpf zebrafish after staining with calcein; Arrows indicate opercle and arrowheads indicate developing centra. Scale bar = 200 μm in A (applies to A′, a, a′, B, B′, b, b′); scale bar = 500 μm in C(applies to C′, c, c′).

Fluorescence occurring in the yolk sac of zebrafish larvae was considered as non-specific as a fluorescence signal was detected in both drug-treated groups as well as in drug-free controls (data not shown).

Spectrophotometric measurements of fluorescence elicited by icaritin and its derivatives in a cell-free environment *in vitro*

Flavonols, with a 3-hydroxyflavone backbone such as quercetin and morin, are reported to exhibit fluorescent properties. For example, one *in vitro* experiment showed that quercetin elicited fluorescence through binding of aluminium ions to the carbonyl and 3-hydroxyl groups.[16] In another study, quercetin-induced fluorescence in the presence of albumin from bovine serum (BSA) was increased at alkaline pH.[17] Hence, the factors that influence icaritin-induced fluorescence were investigated. The fluorescent properties of icaritin, icariin (icaritin glycoside) and quercetin were compared at various concentrations of BSA and Ca^{2+} as well different pH values. Fig. 3A shows the fluorescence intensity of different flavonols (all at 10 μM) in the presence of 25 μM BSA and 10 mM $CaCl_2$ at different pHs. Consistent with a previous study,[17] an elevated fluorescence signal at pH 7–7.5 was observed with quercetin (10 μM). Unlike quercetin, icaritin exhibited a dramatic increase in fluorescence intensity by more than 10^3-fold at pH 12. However, icariin failed to emit fluorescence even in the presence of BSA and Ca^{2+} at alkaline pHs. It is important to point out that the chemical structure of icariin differs from icaritin with the absence of a hydroxyl group at C-3 position. Taken together, our results suggest that the 3-hydroxyl group is essential for the fluorescent emission.

Fig. 3B–E illustrates the fluorescence intensity *versus* dose-response curves of icaritin, $CaCl_2$, BSA and the pH values, respectively. Our results demonstrated a positive correlation of icaritin concentrations (10–100 μM) and the fluorescence emission, and a fluorescence intensity of 10^6 was detected at 100 μM icaritin.

Correlation of the chemical structures of icaritin and its derivatives with emission of bone-specific fluorescence in zebrafish larvae

The opercle, the first dermal bone to ossify in the pharyngeal arches, appears at about 3 days post fertilization (dpf) when the embryos hatch into freely swimming larvae, as reported.[18] Formation of the opercle is commonly used as an anatomical indictor for early growth and development of bone. The appearance of fluorescence in the opercle after treatment with the three icaritin's derivatives is in the order of: icaritin > icariin > epimedin C (Fig. 4). It is important to point out that

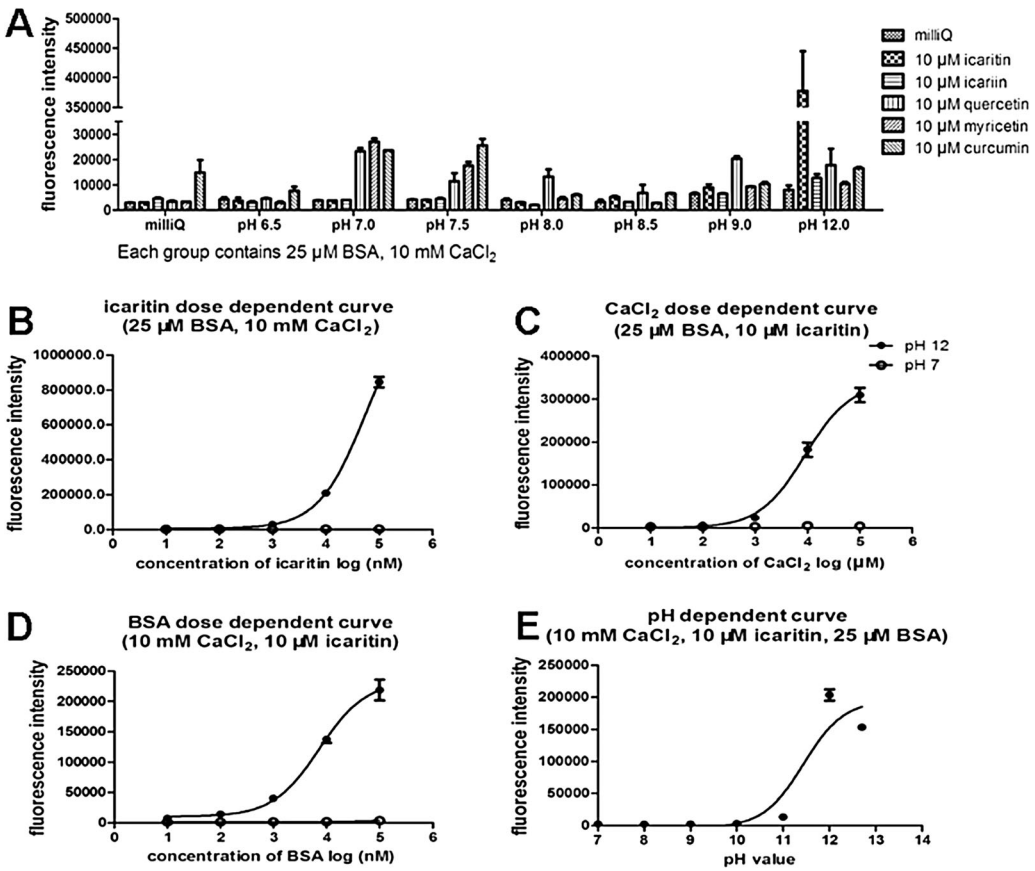

Fig. 3 Fluorescent activity of various flavonoid compounds in the presence of BSA and calcium and at different pH values. A, the fluorescence intensity of different flavonols (all at 10 μM) in the presence of 25 μM BSA, 10 mM $CaCl_2$ at different pH values. Data are plotted as mean ± SEM, (n = 3). B–E, fluorescence intensity *versus* dose-response curves of the different variables; the concentration of icaritin, the concentration of $CaCl_2$, the concentration of BSA and the pH value, respectively. Data are plotted as mean ± SEM (n = 3).

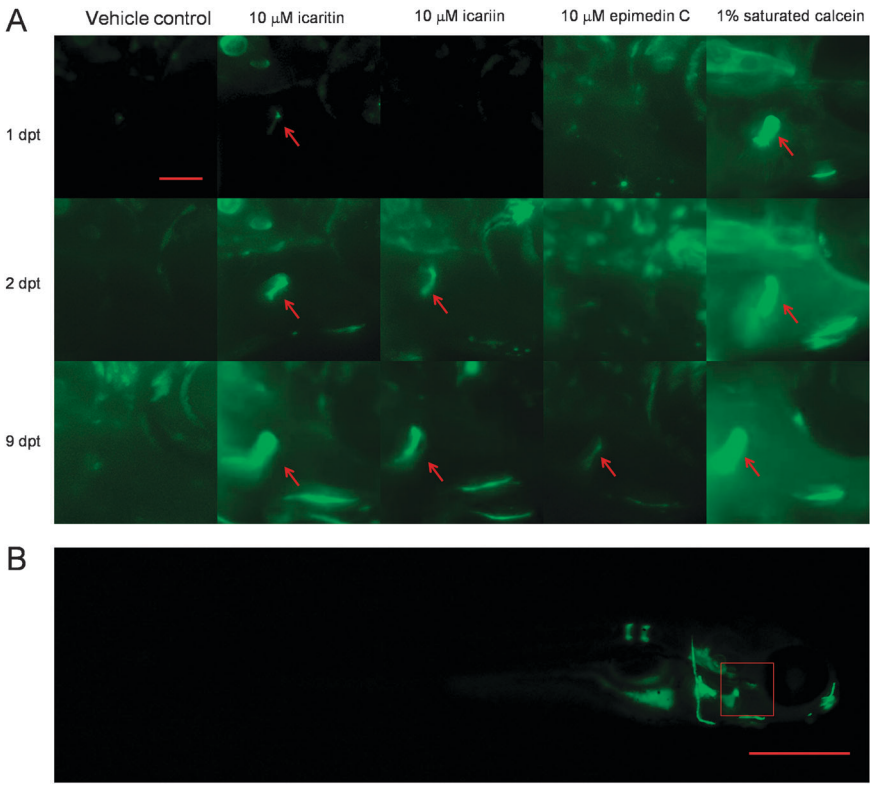

Fig. 4 Appearance of fluorescence in the bone of zebrafish after treatment with icaritin and its derivatives for 1, 2 and 9 days. A, the 5 dpf zebrafish were treated with 0.1% dimethyl sulfoxide (DMSO), Icaritin, Icariin, Epimedin C or 1% saturated calcein (pH 7.0–7.5) solution for 1, 2, or 9 days, respectively (red arrows indicate opercle). B, the lateral view of the whole body of calcein stained 14 dpf zebrafish. Red box indicates the observed area in Fig. 4A. Scale bar = 100 μm in A; scale bar = 500 μm in B.

the differential time of appearance of fluorescence in the opercle is probably negatively correlated with the number of sugar groups found in the chemical structures of icaritin's derivatives in which icariin and epimedin C have two and three sugar moieties, respectively, attached to the aglycoside icaritin.

LC-MS/MS analysis of *in vivo* drug metabolism of icaritin and its derivatives in zebrafish larvae

Our results illustrated that the magnitude of fluorescence intensity in bone of zebrafish larvae increased in the order of: icaritin > icariin > epimedin C (Fig. 4). Intriguingly, in our study icaritin but not icariin emitted fluorescence in a cell-free environment (Fig. 3). It was reported that epimedin C can be metabolized to icariin and subsequently to icaritin in mammalian systems.[19] Thus, it is possible that, in our study, metabolism of icariin and epimedin C occurred which is responsible for the occurrence of fluorescence in bone of zebrafish larvae. The possibility of the occurrence of drug metabolism was determined and compared in zebrafish larvae at 1 day post treatment with these compounds (dpt) and 9 dpt. Interestingly, at 1 dpt, the fluorescence signal of bone was detected only in icaritin-treated zebrafish larvae. At 9 dpt, the fluorescence signal was observed in all treatment groups, and icaritin elicited a stronger fluorescence signal than icariin, and the weakest fluorescence signal one was epimedin C (Fig. 4A).

Drug metabolites profiling of icaritin and its derivatives in zebrafish larvae were performed using targeted product ion analysis, in which ions at m/z 369.1 (parent ion of protonated icaritin) and m/z 313.1 (fragment after loss of isobutene from prenyl group of icaritin) were used as diagnostic ions for the extraction of dependent MS/MS spectra of drug metabolites and the conjugates were identified according to the characteristic neutral loss. For example, a typical MS/MS spectrum of a metabolite at m/z 720.9 that belonged to di-glucuronidated icaritin is shown in Fig. 5A. The successive neutral loss of 176 in the MS/MS spectrum represents the presence of two hydroxyl-linked glucuronide moieties.

Table 1 summarizes the retention time and mass-to-charge ratio of metabolites found in zebrafish larvae after treatments with icaritin, icariin and epimedin C at 1 dpf and 3 dpf. In general, the metabolic reactions involved were mono- and di-glucuronidation (as represented by a nominal mass shift of +176 and +352, respectively), mono-glucosylation (+162), sulfation (+80) and xylation (+146). More metabolites were identified in zebrafish larvae at 3 dpt compared to that in zebrafish larvae at 1 dpt. Our results clearly illustrate that the degree of metabolites conjugation was related to the number of free hydroxyl groups present, and thus different isomers of metabolites were detected. For instance, three isomers of mono-glucuronidated (eluted at 38.8 min, 40.3 min and 41.5 min) and di-glucuronidated icaritin (eluted at 28.8 min, 32.8 min and 33.3 min) were successfully detected.

The majority of metabolites found in icariin and epimedin C-treated zebrafish larvae at 3 dpt were various glucuronidated forms of icaritin, which strongly suggested that icariin and

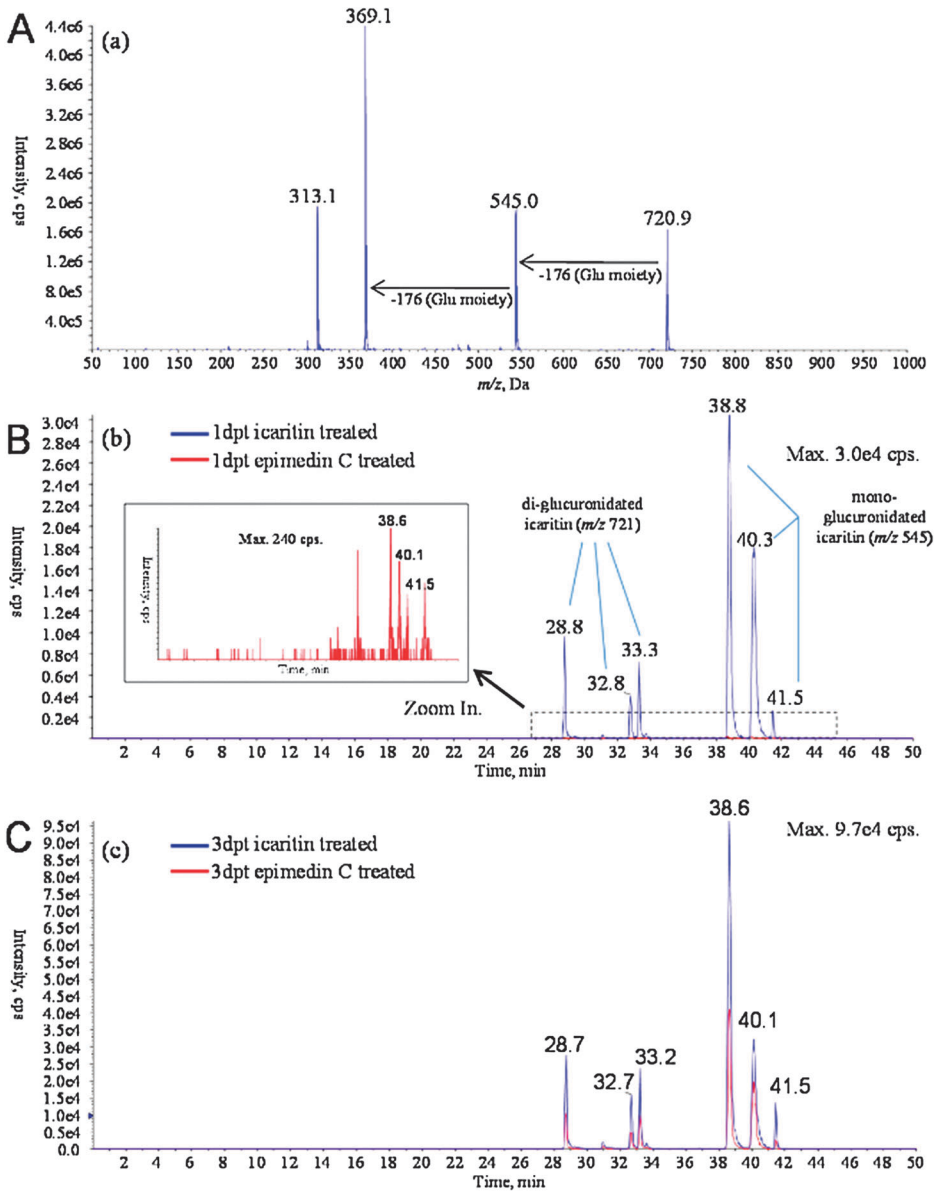

Fig. 5 Study of the metabolism of icaritin and its derivatives in zebrafish larvae. The 5 dpf zebrafish were treated with 0.1% DMSO, 10 μM icaritin, 10 μM icariin or 10 μM epimedin C for one or three days, then larvae were homogenized in 80% (v/v) methanol and prepared for LC-MS/MS analysis. A, typical MS/MS spectrum of metabolites of icaritin (*m*/*z* 369.1), which belonged to di-glucuronidated icaritin at *m*/*z* 720.9 and mono-glucuronidated icaritin at *m*/*z* 545.0. B and C, metabolites identified in 1 dpt and 3 dpt zebrafish larvae, respectively (blue line, icaritin-treated; red line, epimedin C-treated). Because there is a greater discrepancy between icaritin and epimedin C-treated zebrafish larvae, we present data of these two groups for comparison.

epimedin C are normally metabolized *in vivo* to icaritin before conjugation. An ion at *m*/*z* 661.1, which was found in epimedin C-treated zebrafish larvae (1 dpt), probably originated from de-glucosylation of epimedin C which suggests the occurrence of metabolic conversion of epimedin C to icaritin. Fig. 5B and C show the overlaid-extracted ion chromatographs of mono- and di-glucuronidated icaritin obtained from LC-MS/MS experiments. Our results demonstrate that metabolites of icaritin could not be detected in 1 dpt epimedin C-treated zebrafish larvae until these larvae are 3 dpt. These findings indicate that the metabolism of icariin and epimedin C to icaritin in zebrafish and mammalian systems is highly conserved.

Transcriptome analysis of drug metabolism enzymes in zebrafish larvae

So far, our results clearly demonstrated the formation of icaritin and its derivative metabolites in zebrafish larvae. However, it is essential to determine in zebrafish larvae the existence and the abundance of drug metabolizing enzymes essential for the drug metabolic process. Thus, mRNAs harvested from 3 independent batches of zebrafish larvae were isolated for the preparation of three libraries for the subsequent deep sequencing analysis. Tag sequences of the libraries were mapped to the zebrafish transcript datasets of the vertebrate genome annotation (VEGA), UniProt/NCBI and Ensembl

Table 1 A summary of the retention time and mass-to-charge ratio (m/z) of metabolites found in icaritin, icariin and epimedin C-treated zebrafish larvae at 1 dpt and 3 dpt. A tick indicates metabolites were identified in drug-treated zebrafish larvae and a blank indicates no metabolite was detected.

			1 dpt			3 dpt		
Drug metabolite	m/z	Retention time	Icaritin	Icariin	Epimedin C	Icaritin	Icariin	Epimedin C
Icaritin + Glc	531.1	39.2	✓			✓	✓	
Icaritin + Glc + Xyl	677	30.2	✓	✓				
Icaritin + GLc + SO_3	610.9	29				✓		
Icaritin + Glu	545	38.8,40.3,41.5	✓	✓		✓	✓	✓
Icaritin + 2 × Glu	721	28.8,32.8,33.3	✓	✓		✓	✓	✓
Icaritin + Glu + Glc	707	28.9,3.6				✓	✓	✓
Icaritin + Glu + SO_3	625	29.4,31.0				✓		
Icaritin + Glu + Xyl	691.1	30.2,34.8				✓	✓	✓
Icaritin + Xyl	515.1	41.7		✓			✓	
Epimedin C–Glc	661.1	39.2			✓			✓
Epidemin C–Glc–Xyl + Glu	691.1	30.1						✓

databases by MAQ (version: 0.7.1). A total of 4.4 million tag sequences from sequencing of the libraries were found to match with annotated genes of the databases. Of these, 2867 tag sequences were found to be drug metabolism enzymes and these sequences were identified as 51 non-redundant genes encoding key enzymes for drug metabolism. For example, the cytochromes P450 family members, flavin-containing monooxygenase and epoxide hydrolase are involved in phase I drug metabolism, whereas UDP-glucuronosyltransferases, sulfotransferasescatechol-*O*-methyltransferase and glutathione S-transferases are involved in phase II drug metabolism. The relative expression levels of the genes that encode these enzymes were reflected by the number of mapped tags for each annotated gene (Fig. 6). Table 2 summarized the transcriptome data of the landscape of drug metabolism enzymes present in zebrafish larvae.

Proteomic analysis of drug metabolism enzymes in zebrafish larvae

SCX-RP-RP-2D-LC-MS/MS was performed (using an ABI Sciex QStar XL mass spectrometer) as described in "Materials and Methods" in order to generate the proteomic profiles of zebrafish larvae for further identification of the drug metabolism enzymes at the protein level. A total of 2998 distinct proteins were identified by the analysis of mass spectra in two independent protein profiling experiments. The spectra were searched against the International Protein Index 3.56 zebrafish database using the ProteinPilot software and three of these distinct proteins were identified as drug metabolism enzymes (glutathione *S*-transferase M, glutathione *S*-transferase theta 1b and glutathione-S-transferase pi) that belong to the glutathione-*S*-transferases, which are the major phase II detoxification enzymes (Fig. 7).

Discussion

Herba Epimedii, is widely used in China as a medicinal herb for the treatments of skeletal diseases, but has also been shown to have great potential in the prevention and treatment of bone diseases in various experimental models, including ovariectomized rat and rabbit models *in vivo* and in postmenopausal women.[3,6,20] A number of unique flavonoids, including icaritin, icariin and epimedin C, have been identified as the major active constituents in *Herba Epimedii*. However, we do not know whether these compounds act directly or indirectly in bone to produce beneficial effects, and how these compounds are absorbed, metabolized and distributed in bone after consumption remains unclear. In this study, we demonstrated that aglycoside icaritin, but not its glycoside derivative, emitted fluorescence of different intensities under different conditions such as different concentrations of BSA and calcium, as well as pH values of the medium. The fluorescent property of icaritin offers the advantages of observing its distribution directly in live zebrafish larvae *in vivo*. Zebrafish larvae treated with these flavonoids showed a decreasing rate of the appearance of fluorescence signals in the order of icaritin > icariin > epimedin C, which led us to further explore the drug metabolism profiles of these compounds in zebrafish larvae. LC-MS/MS analysis suggested that epimedin C is converted to icariin which is further metabolized to icaritin in zebrafish larvae. Additionally, a total of 51 drug metabolism enzymes involved in the metabolism of icaritin and its glycoside derivatives in zebrafish larvae were identified using transcriptomic and proteomic profiling by deep sequencing and RP-RP-2D-LC-MS/MS, respectively.

An earlier study reported that the flavonoid quercetin could elicit fluorescence through the binding of a metal ion at the carbonyl and 3-hydroxyl groups in the presence of BSA at alkaline pH.[16] In fact, quercetin, icaritin and icaritin glycoside are flavonols (a sub-category of flavonoids) that have a 3-hydroxyflavone backbone. We conducted a series of spectrophotometric analyses to determine the fluorescence activities of icaritin and its glycoside derivative icariin in the presence of BSA and calcium at different pH values. Our results showed that, similar to quercetin, the fluorescence intensity of icaritin is influenced by the concentrations of BSA, Ca^{2+} and the alkaline environment. In contrast, no fluorescence signal could be detected with icariin under similar conditions. Taken together, our results strongly suggests that the hydroxyl group at the C-3 position is essential for fluorescence emission, whereas the presence of glycosides at the same position is unfavorable for fluorescence emission. Although the generation of fluorescence of icaritin and quercetin appears to be similar, there was a $>10^3$-fold increase in fluorescence intensity of icaritin (10 μM) at a pH value of 12 which was not observed with other flavonols tested.

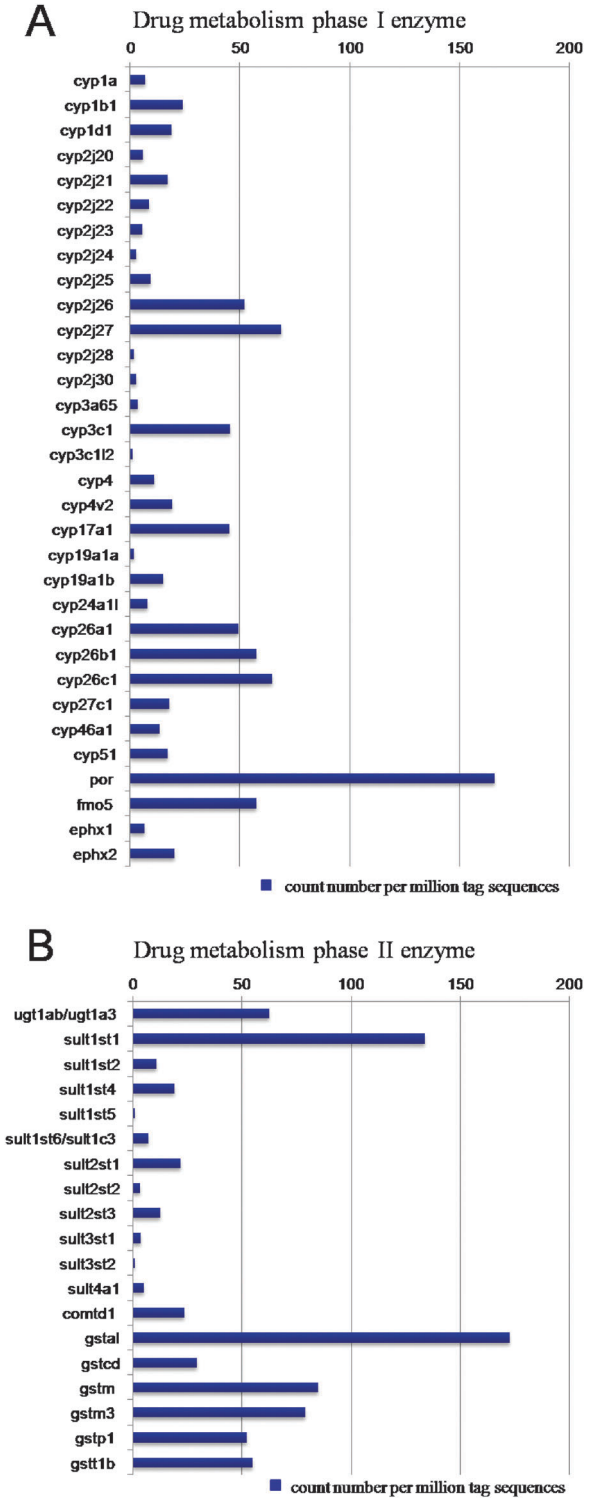

Fig. 6 Identification of drug metabolism enzymes in zebrafish larvae by transcriptome analysis of deep sequencing data. Relative gene expression of the phase I and phase II metabolism enzymes in zebrafish larvae are reflected by the number of mapped tags (per million) for each annotated gene.

The fluorescence properties of icaritin offer the advantage to visualize the dynamic distribution of this flavonoid in the bone of living zebrafish larvae, *in vivo*, directly using fluorescence microscopy. Zebrafish larvae treated with icaritin and its glycoside derivatives icariin and epimedin C, exhibited "bone-specific fluorescence" in a time-dependent manner. Therefore, our results suggested that metabolism of icaritin glycoside derivatives to an aglycoside form occurred, which resulted in bone-specific fluorescence in zebrafish larvae. To further strengthen our conclusion on icaritin metabolism, zebrafish larvae were treated with these compounds at different time points for LC-MS/MS analysis. Metabolites including mono- and di-glucuronidation, mono-glucosylation, sulfation and xylation were identified in zebrafish larvae at 1 dpt and 3 dpt after treatments with icaritin, icariin and epimedin C. The majority of drug metabolites found in icariin- and epimedin C (glycoside forms)-treated zebrafish larvae (3 dpt) were icaritin metabolites (aglycoside forms). Hence, metabolism of icariin and epimedin C involved the cleavage and removal of glycoside groups before conjugation in zebrafish larvae *in vivo*. Moreover, further identification of these conjugated metabolites suggests that phase II drug metabolism occurs during flavonol metabolism in zebrafish larvae. To summarize, the metabolic pathway of epimedin C → icariin → icaritin in zebrafish larvae (this work) and the previously reported similar pathway in mammalian models is highly conserved. The observation of fluorescence of icaritin glycoside derivatives, icariin and epimedin C, in zebrafish larvae *in vivo* but not *in vitro*, as well as the delayed appearance of fluorescence in bone with increasing glycoside groups present in icaritin derivatives, strongly suggests the occurrence of metabolism, *in vivo*, of icaritin glycoside derivatives to icaritin in zebrafish larvae.

In this study, our results clearly illustrates that the metabolic pathway involved for icaritin and its glycoside derivatives in zebrafish larvae is similar to that previously reported in mammals (Fig. 8). Thus, the first step is the enzymatic removal of the sugar moiety of these compounds after consumption in the cells of the gastrointestinal mucosa or it can be removed by enzymes secreted by the colon flora.[21–23] After hydrolysis of the flavonoid derivative to free aglycone, flavonoid aglycone is conjugated by sulfation, glucuronidation, methylation or in different combinations with steps which are controlled by phase II metabolism enzymes (*e.g.* UDP-glucuronosyltransferases, sulfotransferases, catechol-*O*-methyltransferases and glutathione-*S*-transferases). The formation of conjugates can dramatically change the physiochemical and biological properties of the circulating metabolites in the zebrafish body which plays an important role in the biotransformation of flavonoid to more easily excretable forms as well as in the metabolic inactivation of pharmacologically active compounds.[24]

In order to investigate whether zebrafish larvae express the essential drug metabolizing enzymes involved in the proposed metabolic pathways of icaritin and its glycoside derivatives, we used combined transcriptomic and proteomic approaches to determine the identity and the relative expression levels of these enzymes. In fact, transcriptomic profiling procedures identified 51 unique mRNA transcripts (out of a total of 13 310 non-redundant mRNA transcripts) which belong to three categories of key enzymes involved in phase I drug metabolism[25] including the cytochrome P450 families, flavin-containing monooxygenases and epoxide hydrolases in zebrafish larvae. Moreover, mRNA transcripts of several key phase II drug

Table 2 Drug metabolism enzymes identified. A summary of the enzymes identified in 3dpf zebrafish larvae by transcriptome and/or proteome analysis. A tick indicates that enzymes were detected in zebrafish larvae and a blank indicates no enzyme was identified.

	Gene symbol	Nucleotide acc. no.	Protein acc. no.	Transcriptome	Proteome
(A) Phase I enzyme					
Cytochromes P450	Cyp1a	NM_131879	NP_571954	✓	
	Cyp1b1	NM_001045256	NP_001038721	✓	
	Cyp1d1	NM_001007310	NP_001007311	✓	
	Cyp2j20	XM_001337745	XP_001337781	✓	
	Cyp2j21	NM_201511	NP_958919	✓	
	Cyp2j22	NM_200620	NP_956914	✓	
	Cyp2j23	NM_001083035	NP_001076504	✓	
	Cyp2j24	NM_001083049	NP_001076518	✓	
	Cyp2j25	NM_200139	NP_956433	✓	
	Cyp2j26	NM_001009890	NP_001009890	✓	
	Cyp2j27	NM_001025554	NP_001020725	✓	
	Cyp2j28	NM_152954	NP_694486	✓	
	Cyp2j30	NM_001007356	NP_001007357	✓	
	Cyp3a65	NM_001037438	NP_001032515	✓	
	Cyp3c1	NM_212673	NP_997838	✓	
	Cyp3c112	NM_001007400	NP_001007401	✓	
	Cyp4	NM_199216	NP_954686	✓	
	Cyp4v2	NM_001077602	NP_001071070	✓	
	Cyp17a1	NM_212806	NP_997971	✓	
	Cyp19a1a	NM_131154	NP_571229	✓	
	Cyp19a1b	NM_131642	NP_571717	✓	
	Cyp24a11	NM_001089458	NP_001082927	✓	
	Cyp26a1	NM_131146	NP_571221.2	✓	
	Cyp26b1	NM_212666	NP_997831	✓	
	Cyp26c1	NM_001029951	NP_001025122	✓	
	Cyp27c1	NM_001113337	NP_001106808	✓	
	Cyp46a1	NM_001020522	NP_001018358	✓	
	Cyp51	NM_001001730	NP_001001730	✓	
	Por	NM_001034982	NP_001030154	✓	
Flavin containing monooxygenase	Fmo5	NM_198910	NP_944592	✓	
Epoxide hydrolase	Ephx1	NM_201068	NP_957362	✓	
	Ephx2	NM_001008642	NP_001008642	✓	
(B) Phase II enzyme					
UDP-glucuronosyltransferase	Ugt1ab/ugt1a3	NM_213422	NP_998587	✓	
	Sult1st1	NM_182941	NP_891986	✓	
	Sult1st2	NM_183347	NP_899190	✓	
	Sult1st4	NM_205620	NP_991183	✓	
	Sult1st5	NM_045154	NP_001186832	✓	
	Sult1st6/sult1c3	NM_001002599	NP_001002599	✓	
	Sult2st1	NM_198914	NP_944596	✓	
	Sult2st2	NM_001078169	NP_001071367	✓	
	Sult2st3	NM_001078168	NP_001071636	✓	
	Sult3st1	XM_682056	XP_687148	✓	
	Sult3st2	NM_001079947	NP_001073416	✓	
	Sult4a1	NM_001040244	NP_001035334	✓	
Catechol-*O*-methyltransferase	Comtd1	NM_001163808	NP_001157280	✓	
Glutathione *S*-transferase	Gsta1	NM_213394	NP_998559	✓	
	Gstcd	NM_001024462	NP_001019633	✓	
	Gstm	NM_212676	NP_997841	✓	✓
	Gstm3	NM_001162851	NP_001156323	✓	
	Gstp1	NM_131734	NP_571809	✓	✓
	Gst1b	NM_200584	NP_956878	✓	✓

metabolism enzymes,[24] including UDP-glucuronosyltransferase, sulfotransferases, catechol-*O*-methyltransferase and glutathione-*S*-transferases, were identified. However, the proteomic approach only identified three proteins (out of 2998 distinct proteins) which belong to the glutathione-*S*-transferases, a major type of phase II detoxification enzymes. The discrepancy of our results obtained from transcriptomic and proteomic approaches suggest that transcriptomics could provide a "more unbiased" landscape of mRNA expression profile.[26,27] In fact, results from a previous study[28] have suggested that protein identification using proteomic analysis could be greatly influenced by various complicated intrinsic properties of proteins such as hydrophobicity and sub-cellular localization. In addition, the differences observed could be attributed to different half-lives of mRNAs, protein accumulation and degradation kinetics.[29] Therefore, utilization of integrated transcriptomics and proteomics could provide more confirmatory evidence for the identification of drug metabolizing enzymes expressed in zebrafish larvae.

It is important to point out that zebrafish have become one of the most popular vertebrate for drug screening as well as pharmacological and toxicological tests.[30,31] Our results, for the first time, indicate that the zebrafish larvae exhibited a high degree of conservation with mammalian models

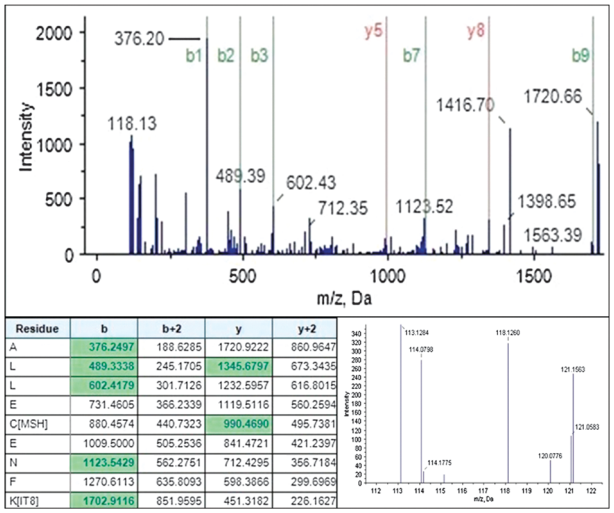

Residue	b	b+2	y	y+2
A	376.2497	188.6285	1720.9222	860.9647
L	489.3338	245.1705	1345.6797	673.3435
L	602.4179	301.7126	1232.5957	616.8015
E	731.4605	366.2339	1119.5116	560.2594
C[MSH]	880.4574	440.7323	990.4690	495.7381
E	1009.5000	505.2536	841.4721	421.2397
N	1123.5429	562.2751	712.4295	356.7184
F	1270.6113	635.8093	598.3866	299.6969
K[IT8]	1702.9116	851.9595	451.3182	226.1627

Fig. 7 A typical MS/MS spectra matched to the fragmentation of peptide ALLECENFK derived from tryptic digestion of protein Glutathione-*S*-transferase pi with a confidence score of 99% and its reporter ion intensity from the control group and the perturbed group. There are six spectra contributing to the quantification of this specific protein.

of the drug metabolism systems. The zebrafish genome sequence is available and the zebrafish is amenable to high-throughput genetic and drug screening.[29] Unfortunately, in the literature, in-depth and systematic drug metabolism/pharmacological studies using zebrafish have been lacking until recently.[32] Nonetheless, the proof-of-concept of the high-level conservation of drug metabolism between zebrafish and mammals, as reported in our present study, strongly supports the usefulness of zebrafish as a vertebrate model for the above-mentioned investigations.

In conclusion, our results demonstrate, for the first time, the distribution of icaritin- and its glycoside derivatives in the bone tissues of zebrafish larvae after treatment by measuring the bone-specific fluorescence signals. Fluorescence emission by icaritin- and its glycosides are caused by the binding to Ca^{2+} ions with its carbonyl and 3-hydroxyl groups in the presence of protein (*e.g.* BSA). Our findings on tracing the drug distribution in zebrafish larvae by live imaging, drug metabolites profiling by LC-MS/MS and identification of drug metabolism enzymes by omic analysis illustrates that the metabolism of icaritin and its derivatives in zebrafish larvae and mammalian models are highly conserved.

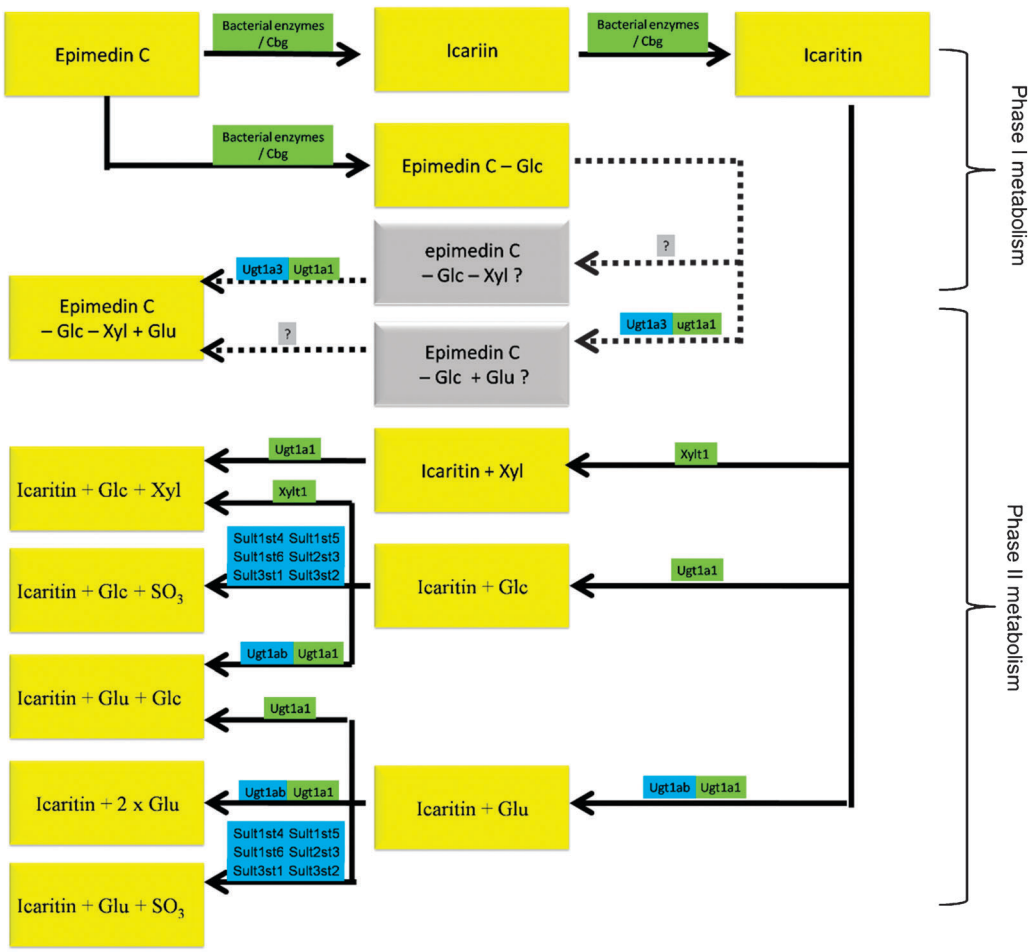

Fig. 8 Proposed metabolism of icaritin, icariin and epimedin C in zebrafish larvae. Metabolites in yellow boxes are identified by LC-MS/MS analysis; enzymes in blue indicate gene/protein identified in present study using transcriptome and/or proteome analysis; enzymes in green indicate genes that were not detected in this study but were found in the NCBI gene database. Metabolic processes in gray boxes are uncertain.

Materials and methods

Ethics statement

All animal experiments were conducted in accordance with the ethical guidelines of the Institute of Chinese Medical Sciences, University of Macau and the protocols were approved by ICMS, University of Macau.

Maintenance of zebrafish and collection of larvae

Adult zebrafish were maintained at a temperature of 28 °C with a 14 h light/10 h dark cycle. Fish were fed twice daily with brine shrimp, and occasionally with commercially available tropical fish food obtained from a local pet shop. Zebrafish eggs were collected in the morning and immersed in water at 28.5 °C,[33] and the zebrafish larvae were subsequently kept in distilled water.

Live imaging of zebrafish larvae by fluorescence microscopy

Fish larvae were anesthetized with 0.016% (w/v) tricaine (Sigma-Aldrich, USA) and observed for morphological changes using a spinning disk confocal microscope system (Olympus IX81 Motorized Inverted Microscope, Japan) equipped with a digital camera (DP controller, Soft Imaging System, Olympus, Japan) or with a stereoscopic zoom microscope (SMZ1000, Nikon, Japan). Images were analyzed with SlideBook 4.2.

Bone staining

For bone staining, live zebrafish larvae were immersed in 1% saturated calcein (pH 7.0–7.5) in Petri dishes for 3–10 min, rinsed three times in MilliQ water and soaked for 10 min so as to remove the excess calcein out of the tissues. Fish were then mounted on 3.5% methylcellulose and observed under the fluorescence microscope with a green fluorescent protein (GFP) filter.

Quantification of fluorescence levels by spectrophotometry in a cell-free environment

The fluorescence signals elicited by calcium/protein/flavonoid interactions was determined in black plates (opaque 96-well microplates, OptiPlate) at a wavelength of 545 nm (excitation at 485 nm). The reaction mixture (200 μL/well) was made in MilliQ water with 1% (v/v) DMSO. The solution was incubated for 5 min at room temperature before the intensity of fluorescence signals was quantified in a fluorescence multi-label counter (Wallac VICTOR-3, PerkinElmer).

Transcriptome analysis

Total RNA was extracted from 30 zebrafish larvae at 3 dpf using the RNeasy Mini Kit (Qiagen, Valencia, CA, USA) in accordance with the manufacturer's instructions. DEGseq, an R package that can handle gene analysis of RNA-seq and microarray data analysis, was used to match gene expression levels in zebrafish larvae.

Pair-ended RNA-seq data were obtained from Beijing Genome Institute (PR of China) in Solexa pipeline version 1.3 formats. The zebrafish genome sequence (Dr6zv8) and annotation file were downloaded from the VEGA database (http://vega.sanger.ac.uk/index.html). Cross-database association information was obtained from the ZFIN online database (http://zfin.org/cgi-bin/webdriver?MIval=aa-ZDB_home.apg).

To perform un-gapped alignment, the mapping software MAQ (version: 0.7.1) was used to map PE short reads. Gene expression levels are counted by the number of mapped reads for each gene.

Proteomic analysis

Several steps are essential for an accurate proteomic analysis of zebrafish larvae. They are total protein extraction, trypsin digestion and labeling, SCX chromatography, on-line RP-RP-2D-LC-MS/MS detection, MS/MS data analysis and identification of sequences and function.

For trypsin digestion and labeling, 100 μg of 200 zebrafish larvae's lysate were reduced in volume to approximately 20 μL, followed by denaturation with SDS, reduction and methylthiocysteine-blocking using the reagents provided and following the protocols as mentioned in the iTRAQ reagents kit. The proteins were digested with 1 : 33 sequencing-grade trypsin at 37 °C overnight. The samples were then labeled at room temperature for 2 h with the appropriate tags following the kit instructions. For SCX chromatography, the combined iTRAQ samples were diluted 13 times into approximately 4 mL of 10 mM H_3PO_4/KH_2PO_4 and 20% Acetonitrile at pH 3 before SCX fractionation with a Perkin Elmer series 200 LC system on a PolySULFOETHYL A™ column (100 mm × 2.1 mm, 5 μm, 300A). The eluate was monitored with an Agilent 1100 diode-array detector module (Agilent Technologies; Santa Clara, CA) (UV absorption at 220 nm with a bandwidth of 6 nm). The SCX fractions were separated by on-line high-pH RP-RP-2D-LC for on-line RP-RP-2D-LC-MS/MS analysis. Briefly, from each 100 μL of SCX eluate, 40 μL were injected for MS/MS analysis. The solvents used for high-pH RP and low-pH RP separation were driven by two separate Agilent 1100 capillary LC pumps (Agilent Technologies; Santa Clara, CA) at a flow rate of 1.5 μL min^{-1}. The low-pH RPLC eluates were coupled online to a QSTAR XL quadrupole time-of-flight hybrid mass spectrometer (Applied Biosystems; Foster City, CA) through an electrospray interface. The MS/MS data were analyzed directly using the Paragon algorithm in the ProteinPilot 2.0.1 software (AppliedBiosystems, Foster City, CA). The MS/MS spectra were matched against theoretical spectra generated from sequences in the International Protein Index release 3.56 *Danio rerio* (43 489 entries) protein database (http://www.uniprot.com).

Drug administration and metabolic study of drugs

For the *in vivo* study of drug metabolism, 200 healthy zebrafish larvae were selected at 5 dpf and placed into a 12-well microplate. Milli-Q water was blotted from the microplate wells and solutions containing either icaritin or one of its glycoside derivatives were added to the wells at serially diluted concentrations immediately. Larvae treated in individual wells were incubated at 28 °C for 1–9 days depending on the nature of assays. The drug-treated larvae were put into 0.5 mL of 80% (v/v) methanol, homogenized and then centrifuged at 150 000 g for 30 min at 20 °C. The supernatants were collected for the detection of drug metabolites with an LC-MS/MS system

consisting of an API 2000 Qtrap hydrid QqQ-linear ion-trap mass spectrometer equipped with TurboIonSpray® source (Applied Biosystems, Foster City, CA) and an HP 1100 series HPLC system (Agilent Technologies, Palo Alto, CA) equipped with a ZORBAX SB–C_{18} column (2.1 mm × 150 mm, 3.5 μm particle size; Agilent Technologies, Palo Alto, CA). Separation was done with a mobile phase of 0.5% (v/v) acetic acid (A) and acetonitrile (B), with a linear gradient of 30%–65% B over 35 min. The flow rate was maintained at 200 μL min^{-1} with the pneumatically assisted electrospray probe using high-purity nitrogen gas (purity ~99.995%) as the nebulizing gas and heating gas. Optimized MS conditions were as follows: ion spray voltage, 5.5 kV; nebulizing gas, 50 (arbitrary units); heating gas, 40 (arbitrary units); curtain gas, 20 (arbitrary units); source temperature, 400 °C; collision gas, 5 (arbitrary units); declustering potential, 20 V; entrance potential, 10 V. The information-dependent acquisition threshold was set at 1.0×10^5 counts per second, above which enhanced product ion spectra were collected from the three most intense peaks with a scan rate of 4000 atomic mass unit (amu)/s. The resolution of Q1 was set at low and the scan range was 200–1000 amu. Data acquisition was interfaced to a computer workstation running Analyst1 1.4.2 (Applied Biosystems).

Chemicals

Icaritin (purity ~98%) and icariin (purity ~98%) were obtained from Yifang Chemical Company (Tianjing, PR of China). Epimedin C (purity ~98%) was purchased from the Ronghe Chemical Company (Shanghai, PR of China). Quercetin (purity ~98%) was purchased from the National Institute for the Control of Pharmaceutical and Biological Products (Beijing, PR of China). BSA was purchased from Sigma-Aldrich (St. Louis, USA).

Statistics

Data were expressed as mean ± SEM of individual experiments. Statistical comparisons were performed using one-way ANOVA, followed by Tukey's least significant difference *t*-test for post hoc analysis (GraphPad software, San Diego, USA). Statistical significance was set at $P < 0.05$.

Acknowledgements

This study is supported by a grant from the Science and Technology Development Fund of Macau SAR (Ref. No. 045/2007 and Ref. No. 058/2009) and Research Committee, University of Macau (UL017) and BMRC grant from A-STAR, Singapore (grant number 07/1/21/19/544). The authors state no conflict of interest.

References

1 F. Xie, C. F. Wu, W. P. Lai, X. J. Yang, P. Y. Cheung, X. S. Yao, P. C. Leung and M. S. Wong, *Evidence-Based Complementary Altern. Med.*, 2005, **2**(3), 353–61.
2 S. Yu, K. Chen, S. Li and K. Zhang, *Chin. J. Dent. Res.*, 1999, **2**(1), 7–11.
3 G. Zhang, L. Qin and Y. Shi, *J. Bone Miner. Res.*, 2007, **22**(7), 1072–9.
4 J. S. Park, H. Y. Park, H. S. Rho, S. Ahn, D. H. Kim and I. S. Chang, *J. Microbiol. Biotechnol.*, 2008, **18**, 110–7.
5 J. P. Yuan, J. H. Wang and X. Liu, *Mol. Nutr. Food Res.*, 2007, **51**, 765–81.
6 G. Zhang, L. Qin, H. Sheng, X. L. Wang, Y. X. Wang, D. K. Yeung, J. F. Griffith, X. S. Yao, X. H. Xie, Z. R. Li, K. M. Lee and K. S. Leung, *Bone*, 2009, **44**(2), 345–56.
7 S. G. Vascotto, Y. Beckham and G. M. Kelly, *Biochem. Cell Biol.*, 1997, **75**, 479–485.
8 C. Parng, W. L. Seng, C. Semino and P. McGrath, *Assay Drug Dev. Technol.*, 2002, **1**, 41–48.
9 J. Y. Tang, S. Li, Z. H. Li, Z. J. Zhang, G. Hu, L. C. Cheang, D. Alex, M. P. Hoi, Y. W. Kwan, S. W. Chan, G. P. Leung and S. M. Lee, *PLoS One*, 2010, **5**(7), e11822.
10 S. Y. Ho, M. Pack and S. A. Farber, *Methods Enzymol.*, 2003, **364**, 408–26.
11 U. Langheinrich, *BioEssays*, 2003, **25**(9), 904–12.
12 T. Suzuki, Y. Takagi, H. Osanai, L. Li, M. Takeuchi, Y. Katoh, M. Kobayashi and M. Yamamoto, *Biochem. J.*, 2005, **388**(Pt 1), 65–73, 15.
13 D. Alex, E. C. Leong, Z. J. Zhang, G. T. Yan, S. H. Cheng, C. W. Leong, Z. H. Li, K. H. Lam, S. W. Chan and S. M. Lee, *J. Cell Biochem.*, 2010, **109**(2), 339–46.
14 J. F. Rawls, B. S. Samuel and J. I. Gordon, *Proc. Natl. Acad. Sci. U. S. A.*, 2004, **101**(13), 4596–601, 30.
15 S. J. Du, V. Frenkel, G. Kindschi and Y. Zohar, *Dev. Biol.*, 2001, **238**(2), 239–46.
16 A. C. Gutierrez and M. H. Gehlen, *Spectrochim. Acta, Part A*, 2002, **58**(1), 83–9.
17 H. O. Gutzeit, Y. Henker, B. Kind and A. Franz, *Biochem. Biophys. Res. Commun.*, 2004, **318**(2), 490–5.
18 C. B. Kimmel, A. DeLaurier, B. Ullmann, J. Dowd and M. McFadden, *PLoS One*, 2010, **5**(3), e9475.
19 P. Shen, S. P. Wong and E. L. Yong, *J. Chromatogr., B: Anal. Technol. Biomed. Life Sci.*, 2007, **857**(1), 47–52, 15.
20 Y. Sun, S. M. Lee, Y. M. Wong, C. P. Lau, L. Qin, P. C. Shaw, P. C. Leung and K. P. Fung, *Phytother. Res.*, 2007, **22**, 267–73.
21 A. Scalbert and G. Williamson, *J. Nutr.*, 2000, **130**(8S Suppl), 2073S–85S.
22 T. Walle, Y. Otake, U. K. Walle and F. A. Wilson, *J. Nutr.*, 2000, **130**(11), 2658–61.
23 T. Walle, *Free Radical Biol. Med.*, 2004, **36**(7), 829–37.
24 P. Jancova, P. Anzenbacher and E. Anzenbacherova, *Biomed. Pap. Med. Fac. Univ. Palacky Olomouc Czech Repub.*, 2010, **154**(2), 103–16.
25 L. L. Brunton, L. S. Goodman, D. Blumenthal, I. Buxton and K. L. Parker, *Goodman and Gilman's manual of pharmacology and therapeutics*, McGraw-Hill Professional, New York, 2007, pp. 43-56.
26 T. Mijalski, A. Harder, T. Halder, M. Kersten, M. Horsch, T. M. Strom, H. V. Liebscher, F. Lottspeich and M. H. de Angelis, *Proc. Natl. Acad. Sci. U. S. A.*, 2005, **102**, 8621–8626.
27 M. De Wit, D. Keil, K. van der Ven, S. Vandamme, E. Witters and W. De Coen, *Gen. Comp. Endocrinol.*, 2010, **167**(2), 190–201.
28 P. S. Hegde, I. R. White and C. Debouck, *Curr. Opin. Biotechnol.*, 2003, **14**(6), 647–51.
29 I. Forné, J. Abián and J. Cerdà, *Proteomics*, 2010, **10**(4), 858–72.
30 T. P. Barros, W. K. Alderton, H. M. Reynolds, A. G. Roach and S. Berghmans, *Br. J. Pharmacol.*, 2008, **154**(7), 1400–13.
31 J. Giacomotto and L. Ségalat, *Br. J. Pharmacol.*, 2010, **160**(2), 204–16.
32 G. J. Lieschke and P. D. Currie, *Nat. Rev. Genet.*, 2007, **8**, 353–367.
33 M. Westerfield, *The Zebrafish Book 4*, The University of Oregon Press, Eugene, Oregon, USA, 2000.

